2012

Holographic field theory models of dark energy in interaction with dark matter

PHYSICAL REVIEW D, COLLEGE PK, v. 85, n. 12, supl. 2, Part 3, pp. 796-800, 44348, 2012
http://www.producao.usp.br/handle/BDPI/40948

PHYSICAL REVIEW D **85,** 123536 (2012)

Holographic field theory models of dark energy in interaction with dark matter

Sandro M. R. Micheletti*

Instituto de Física, Universidade de São Paulo, CP 66318, 05315-970, Sao Paulo, Brazil

(Received 3 October 2011; published 21 June 2012)

We discuss two Lagrangian interacting dark energy models in the context of the holographic principle. The potentials of the interacting fields are constructed. The models are compared with CMB distance information, baryonic acoustic oscillations, lookback time and the Constitution supernovae sample. For both models, the results are consistent with a nonvanishing interaction in the dark sector of the Universe and the sign of coupling is consistent with dark energy decaying into dark matter, alleviating the coincidence problem—with more than 3 standard deviations of confidence for one of them. However, this is because the noninteracting holographic dark energy model is a bad fit to the combination of data sets used in this work as compared to the cosmological constant with cold dark matter model, so that one needs to introduce the interaction in order to improve this model.

DOI: 10.1103/PhysRevD.85.123536 PACS numbers: 98.80.Cq, 95.36.+x

I. INTRODUCTION

In the past years, there have been several papers where an interaction in the dark sector of the Universe is considered [1–6]. A motivation for considering the interaction is that dark energy and dark matter will evolve coupled to each other, alleviating the coincidence problem [1]. A further motivation is that, assuming dark energy to be a field, it would be more natural that it couples with the remaining fields of the theory, in particular, with dark matter, as it is quite a general fact that different fields generally couple. In other words, it is reasonable to assume that there is no symmetry preventing such a coupling between dark energy and dark matter fields. Using a combination of several observational data sets, as supernovae data, CMB shift parameter, baryonic acoustic oscillations (BAO), etc., it has been found that the coupling constant is small but nonvanishing within at least 1σ confidence level [1–4]. In two recent works, the effect of an interaction between dark energy and dark matter on the dynamics of galaxy clusters was investigated through the Layser-Irvine equation, the relativistic equivalent of virial theorem [7]. Using galaxy cluster data, it has been shown that a nonvanishing interaction is preferred to describe the data within several standard deviations [8]. However, in most of these papers, the interaction term in the equation of motion is derived from phenomenological arguments. It is interesting to obtain the interaction term from a field theory. Some works have already taken a step in such a direction [4,6,9]. On the other hand, scalar fields have been largely used as candidates to dark energy. They naturally arise in particle physics and string theory. Good reviews on this subject can be found in [10]. A motivation to use scalar fields as candidates to dark energy is that their pressure can be negative, making it possible to reproduce the recent period of accelerated expansion of the Universe. For example, for a canonical scalar field, the equation-of-state parameter varies between 1 and -1. Dark energy modeled as a canonical scalar field is called quintessence and was investigated, for example, in [9,11]. For a tachyon scalar field, the equation of state is always negative. The tachyon field has been studied in recent years in the context of string theory, as a low-energy effective theory of D-branes and open strings [12]. Tachyon field as dark energy was studied, for example, in [4,13,14]. The first question about scalar fields concerns the choice of the potential. Common choices are the power law and the exponential potentials. However, these choices are in fact arbitrary. In principle, any other form for the potential which leads to recent accelerated expansion would be acceptable.

On the other hand, it is possible that a complete understanding of the nature of dark energy will only be possible within a quantum gravity theory context. Although results for quantum gravity are still missing, or at least premature, it is possible to introduce, phenomenologically, some of its principles in a model of dark energy. Recently, combinations of quintessence, quintom, and tachyon models with holographic dark energy have been proposed—in [15,16,14], respectively. Specifically, by imposing that the energy density of the scalar field must match the holographic dark energy density, namely, $\rho_\Lambda = 3c^2 M_{\rm Pl}^2 L^{-2}$, where c is a numerical constant and L is the infrared cutoff, it was demonstrated that the equation of motion of fields for the noninteracting case reproduces the equation of motion for holographic dark energy. In fact, to impose that the energy density of a scalar field must match the holographic dark energy density corresponds to specify its potential. This can be seen as a physical criterion to choose the potential. Here, we generalize this idea for two kinds of interacting scalar fields.

II. THE MODELS

We consider the general action

$$S = \int d^4x\sqrt{-g}\Big\{-\frac{M_{\rm Pl}^2}{2}R + \mathcal{L}_\varphi(x) + \frac{i}{2}[\bar{\Psi}\gamma^\mu\nabla_\mu\Psi - \bar{\Psi}\bar{\nabla}_\mu\gamma^\mu\Psi] - (M - \beta\varphi)\bar{\Psi}\Psi + \sum_j \mathcal{L}_j(x)\Big\} \quad (1)$$

*smrm@fma.if.usp.br

where $M_{\rm Pl} \equiv (8\pi G)^{-1/2}$ is the reduced Planck mass, R is the curvature scalar, $\mathcal{L}_\varphi(x)$ is, unless of the coupling term, the Lagrangian density for the scalar field, which we will identify with dark energy, Ψ is a massive fermionic field, which we will identify with dark matter, β is the dimensionless coupling constant, and $\sum_j \mathcal{L}_j(x)$ contains the Lagrangian densities for the remaining fields. Notice that, in this work, we will only consider an interaction of dark energy with dark matter. If there was a coupling between the scalar field and baryonic matter, the corresponding coupling constant β_b should satisfy the solar system constraint [17]

$$\beta_b \lesssim 10^{-2}. \tag{2}$$

We assume $\beta_b \equiv 0$, which trivially satisfy the constraint (2).

We consider two kinds of scalar fields: the canonical scalar field, or quintessence field, for which

$$\mathcal{L}_\varphi(x) = \tfrac{1}{2}\partial_\mu\varphi\,\partial^\mu\varphi - V(\varphi), \tag{3}$$

and the tachyon scalar field, for which

$$\mathcal{L}_\varphi(x) = -V(\varphi)\sqrt{1 - \alpha\partial^\mu\varphi\,\partial_\mu\varphi}, \tag{4}$$

where α is a constant with dimension MeV^{-4}. Notice that in both cases, we assume a Yukawa coupling with the dark matter field Ψ.

A. Quintessence field

For the quintessence field, $\mathcal{L}_\varphi(x)$ in the action (1) is given by (3). From a variational principle, we obtain

$$i\gamma^\mu\nabla_\mu\Psi - M^*\Psi = 0, \tag{5}$$

$$i(\nabla_\mu\bar{\Psi})\gamma^\mu + M^*\bar{\Psi} = 0, \tag{6}$$

where $M^* \equiv M - \beta\varphi$, and

$$\nabla_\mu\partial^\mu\varphi + \frac{dV(\varphi)}{d\varphi} = \beta\bar{\Psi}\Psi. \tag{7}$$

Equations (5) and (6) are, respectively, the covariant Dirac equation and its adjoint, in the case of a nonvanishing interaction between the Dirac field and the scalar field φ. For homogeneous fields and adopting the flat Friedmann-Robertson-Walker metric, $g_{\mu\nu} = \mathrm{diag}(1, -a^2(t), -a^2(t), -a^2(t))$, where $a^2(t)$ is the scale factor, Eqs. (5) and (6) lead to

$$\frac{d(a^3\bar{\Psi}\Psi)}{dt} = 0$$

which is equivalent to

$$\bar{\Psi}\Psi = \bar{\Psi}_0\Psi_0\left(\frac{a_0}{a}\right)^3 \tag{8}$$

and (7) reduces to

$$\ddot{\varphi} + 3H\dot{\varphi} + \frac{dV(\varphi)}{d\varphi} = \beta\bar{\Psi}\Psi, \tag{9}$$

where $H \equiv \frac{\dot{a}}{a}$ is the Hubble parameter.

From the energy-momentum tensor, we get

$$\rho_\varphi = \tfrac{1}{2}\dot{\varphi}^2 + V(\varphi), \tag{10}$$

$$P_\varphi = \tfrac{1}{2}\dot{\varphi}^2 - V(\varphi), \tag{11}$$

$$\rho_\Psi = M^*\bar{\Psi}\Psi, \tag{12}$$

$$P_\Psi = 0.$$

From (10) and (11), we have $\omega_\varphi \equiv \frac{P_\varphi}{\rho_\varphi} = \frac{\frac{1}{2}\dot{\varphi}^2 - V(\varphi)}{\frac{1}{2}\dot{\varphi}^2 + V(\varphi)}$. Differentiating (10) and (12) with respect to time and using (8) and (9), we obtain

$$\dot{\rho}_\varphi + 3H\rho_\varphi(\omega_\varphi + 1) = \beta\dot{\varphi}\bar{\Psi}_0\Psi_0\left(\frac{a_0}{a}\right)^3 \tag{13}$$

and

$$\dot{\rho}_\Psi + 3H\rho_\Psi = -\beta\dot{\varphi}\bar{\Psi}_0\Psi_0\left(\frac{a_0}{a}\right)^3, \tag{14}$$

where the dot represents derivative with respect to time.

For baryonic matter and radiation, we have respectively

$$\dot{\rho}_b + 3H\rho_b = 0 \tag{15}$$

and

$$\dot{\rho}_r + 3H\rho_r(\omega_r + 1) = 0, \tag{16}$$

where $\omega_r = \frac{1}{3}$. Equations (15) and (16) imply that $\rho_b(z) = \frac{\rho_{b0}}{a^3}$ and $\rho_r(z) = \frac{\rho_{r0}}{a^4}$, respectively. The subscript 0 denotes the quantities today. We are considering the radiation as composed by photons and massless neutrinos, so that $\rho_{r0} = (1 + 0.2271N_{\rm eff})\rho_{\gamma 0}$, where $N_{\rm eff} = 3.04$ is the effective number of relativistic degrees of freedom and $\rho_{\gamma 0}$ is the energy density of photons, given by $\rho_{\gamma 0} = \frac{\pi^2}{15}T_{\rm CMB}$, being $T_{\rm CMB} = 2.725K$ the CMB temperature today. The Friedmann equation for a flat universe reads

$$H^2 = \frac{1}{3M_{\rm Pl}^2}\left[M^*\bar{\Psi}_0\Psi_0\left(\frac{a_0}{a}\right)^3 + \frac{1}{2}\dot{\varphi}^2 + V(\varphi) + \frac{\rho_{b0}}{a^3} + \frac{\rho_{r0}}{a^4}\right]. \tag{17}$$

In order to determine the dynamics of the interacting quintessence field, it is necessary to specify the potential $V(\varphi)$. Instead of choosing an explicit form for $V(\varphi)$, we will specify it implicitly, by imposing that the energy density of the quintessence field, given by (10), must match the holographic dark energy density, $\rho_\Lambda = 3c^2M_{\rm Pl}^2L^{-2}$, where c is a numerical constant and L is the infrared cutoff. The evolution of the interacting quintessence field with redshift will be given by the equation of evolution for the holographic dark energy density, with a certain expression for the equation-of-state parameter ω_φ. In fact, we will see that imposing the energy density of the quintessence field to match the holographic dark energy density leads to an expression for the potential.

In [18], it has been argued that, in order that holographic dark energy drives the recent period of accelerated expansion, the IR cutoff L must be the event horizon $R_h = a(t)\int_t^\infty \frac{dt'}{a(t')}$. Substituting R_h in the expression of the holographic dark energy, we get $R_h = \frac{c}{H\sqrt{\Omega_\varphi}}$, therefore,

$$\int_t^\infty \frac{dt'}{a(t')} = \frac{c}{a(t)H\sqrt{\Omega_\varphi}}.$$

Differentiating both sides with respect to time, using the Friedmann equation (17) together with conservation equations (13) and (14), we obtain

$$\frac{d\Omega_\varphi}{dz} = -\frac{\Omega_\varphi}{1+z}\left(2\frac{\sqrt{\Omega_\varphi}}{c} + 3\Omega_\varphi\omega_\varphi + \Omega_r + 1\right). \quad (18)$$

Equation (18) is just the equation of evolution for the holographic dark energy [18]. Using the Friedmann equation (17), the conservation equations (15) and (16) can be written as

$$\frac{d\Omega_b}{dz} = -\frac{\Omega_b}{1+z}(3\Omega_\varphi\omega_\varphi + \Omega_r) \quad (19)$$

and

$$\frac{d\Omega_r}{dz} = -\frac{\Omega_r}{1+z}(3\Omega_\varphi\omega_\varphi + \Omega_r - 1). \quad (20)$$

We define $r \equiv \frac{\rho_\Psi}{\rho_\varphi}$. Differentiating r with respect to time, using (13), (14), (10), and (11) we obtain

$$\dot{r} = 3Hr\omega_\varphi - \mathrm{sign}[\dot{\varphi}]\frac{\beta(1+r)}{\sqrt{3}M_{\rm Pl}H}\sqrt{\frac{1+\omega_\varphi}{\Omega_\varphi}}\bar{\Psi}_0\Psi_0\left(\frac{1+z}{1+z_0}\right)^3. \quad (21)$$

We can rewrite $\bar{\Psi}_0\Psi_0$ in terms of observable quantities. In fact, by imposing that the dark matter density today matches the observed value, we obtain $\bar{\Psi}_0\Psi_0 = \frac{3M_{\rm Pl}^2H_0^2(1-\Omega_{\varphi0}-\Omega_{b0}-\Omega_{r0})}{M-\beta\phi_0}$. The sign of $\dot{\varphi}$ is arbitrary, as it can be modified by redefinitions of the field, $\varphi \to -\varphi$, and of the coupling constant, $\beta \to -\beta$. Noticing that $r = \frac{1-\Omega_\varphi-\Omega_b-\Omega_r}{\Omega_\varphi}$, we can substitute r and $\dot{r}$ in (21) by Ω_φ, Ω_b, Ω_r, $\dot{\Omega}_\varphi$, $\dot{\Omega}_b$, and $\dot{\Omega}_r$. Using (18)–(20), we obtain, after some algebra,

$$\omega_\varphi(z) = -\frac{1}{3} - \frac{2\sqrt{\Omega_\varphi}}{3c} + \frac{\gamma(z)}{3}\Bigg[\gamma(z) + \sqrt{\gamma(z)^2 + 4\left(1 - \frac{\sqrt{\Omega_\varphi}}{c}\right)}\Bigg], \quad (22)$$

where

$$\gamma(z) = \frac{1}{\sqrt{2}}\delta M_{\rm Pl}\frac{(1-\Omega_{\varphi0}-\Omega_{b0}-\Omega_{r0})}{E(z)^2\sqrt{\Omega_\varphi}}\left(\frac{1+z}{1+z_0}\right)^3, \quad (23)$$

with

$$E(z) \equiv \frac{H(z)}{H_0} = \sqrt{\frac{[(1-\delta\Delta\varphi)(1-\Omega_{\varphi0}-\Omega_{b0}-\Omega_{r0})+\Omega_{b0}]}{1-\Omega_\varphi}\left(\frac{1+z}{1+z_0}\right)^3 + \frac{\Omega_{r0}}{1-\Omega_\varphi}\left(\frac{1+z}{1+z_0}\right)^4}, \quad (24)$$

where $\Delta\varphi(z) \equiv \varphi(z) - \varphi_0$ and $\delta \equiv \frac{\beta}{M-\beta\varphi_0}$ is an effective coupling constant. Notice that, if $\delta = 0$, (22) reproduces the equation-of-state parameter obtained in [18].

The evolution of the quintessence field is given by

$$\frac{d\varphi}{dz} = -\frac{\sqrt{3}M_{\rm Pl}\sqrt{\Omega_\varphi(z)(1+\omega_\varphi(z))}}{1+z}. \quad (25)$$

From (18)–(20) and (25), we can calculate the evolution with redshift of all observables in the model. If we wish to calculate the time dependence, we need to integrate the Friedmann equation (17), which can be written in the form

$$\frac{dt}{dz} = -\frac{1}{H_0E(z)(1+z)}.$$

From (10), we can compute the potential $V(z)$ as

$$\frac{V(z)}{\rho_{c0}} = \frac{E^2(z)\Omega_\varphi(z)}{2}(1-\omega_\varphi(z)), \quad (26)$$

where $\rho_{c0} = 3M_{\rm Pl}^2H_0^2$, $E(z)$ is given by (24), $\omega_\varphi(z)$ is given by (22), and $\Omega_\varphi(z)$ is the solution of (18). From (26) and (25), we can compute $V(\varphi)$.

Here, it is worth saying that in the holographic dark energy model, in the noninteracting case—(22) with $\delta = 0$—$\omega_\varphi$can be less than -1. However, as already mentioned in [15], if we wish that the holographic dark energy is the quintessence field, then because (25), ω_φ must be more than -1. Nevertheless, in the interacting case considered here, due to the fact that ω_φ depends explicitly on φ, ω_φ cannot be less than -1. On the other hand, the square root in (22) must be real. We can verify that ω_φ is real and $\omega_\varphi > -1$ if (i) $\frac{\sqrt{\Omega_{\varphi0}}}{c} < 1$ or (ii) $\frac{\sqrt{\Omega_{\varphi0}}}{c} > 1$ and $|\delta|M_{\rm Pl} \geq \frac{2\sqrt{2\Omega_{\varphi0}}}{1-\Omega_{\varphi0}-\Omega_{b0}-\Omega_{r0}}\sqrt{\frac{\sqrt{\Omega_{\varphi0}}}{c}-1}$. However, the case (ii) is irrelevant, as it corresponds to large values of $|\delta|M_{\rm Pl}$. For example, if $\Omega_{\varphi0} = 0.7$ and $c = 0.8$, we have $|\delta|M_{\rm Pl} \gtrsim 1.69$. Below, we will see that the

observational data constrain $|\delta| M_{\rm Pl} \sim 10^{-1}$. In order that ω_φ be real for all future times, as $\Omega_\varphi \to 1$, it is necessary that $c \geq 1$.

It is interesting to notice that the condition $\frac{\sqrt{\Omega_{\varphi 0}}}{c} < 1$ is precisely the same one for which the entropy of the Universe increases [18]. As $\Omega_\varphi \to 1$ in the future, it is necessary that $c \geq 1$. Therefore, the condition for ω_φ to be real is precisely the same one for the entropy to increase. So, the model respects the second law of thermodynamics.

In Fig. 1, we see the evolution of the equation-of-state parameter ω_φ with the scale factor a. For the noninteracting case, $\delta = 0$, we have $\omega_\varphi \to -1/3$, as $\Omega_\varphi(z) \ll 1$ for $z \gg 1$. For $\delta < 0$, $\omega_\varphi > -1$ in the matter era, then approaches -1 in the radiation era. For $\delta > 0$, ω_φ will eventually turn out positive and possibly $\omega_\varphi \gg 1$ in very early times, as in the case shown in Fig. 1. This behavior is explained as follows. In the matter era, $E^2(z) \sim (1+z)^3$ so that $\gamma(z) \sim \frac{1}{\sqrt{\Omega_\varphi}}$. From (18), $\frac{d\Omega_\varphi}{dz} < 0$, so $|\gamma(z)|$ increases with redshift. This increasing of $|\gamma(z)|$ will continue until the radiation era, when $E^2(z) \sim (1+z)^4$ and $\Omega_\varphi(z) \sim (1+z)^{-2}$ so that $|\gamma(z)| \to$ const. Typically, this constant will be much more than one. Therefore, for high redshifts $\omega_\varphi(z) \simeq -\frac{1}{3} + \frac{\gamma}{3}[\gamma + |\gamma| + \frac{2}{|\gamma|}]$. If $\delta < 0$, then $\gamma < 0$ and $\omega_\varphi(z) \simeq -1$ in the radiation era. If $\delta > 0$, then $\gamma > 0$ and $\omega_\varphi(z) \simeq \frac{1}{3} + \frac{2}{3}\gamma^2 \to$ const. Notice from (26) that if $\omega_\varphi(z) > 1$ then $V < 0$. In order to avoid it, we impose the condition $\omega_\varphi \leq 1$ for all z. This condition is satisfied if $\delta M_{\rm Pl} \lesssim \frac{\sqrt{2}(1-\Omega_{\varphi 0})}{1-\Omega_{\varphi 0}-\Omega_{b0}}\sqrt{\Omega_\varphi}$. As we have $\Omega_\varphi \ll 1$ as z increase, there will be an abrupt decrease in the positive tail of the probability distribution of δ, as well as in the confidence regions of δ with other parameters.

In Fig. 2, $V(\varphi)$ is shown for some values of δ and c. Notice that there is a region where $V(\varphi)$ is almost constant, that is, there is a slow-roll region. As we chose $\dot\varphi$ positive, then φ evolves to this slow-roll region. However, if we had chosen $\dot\varphi$ negative, then because the right-hand side of (25) would have the opposite sign, so $\frac{dV(\varphi)}{d\varphi}$ would have also the opposite sign and again φ would evolve to the slow-roll region. Notice also that for $\delta M_{\rm Pl} = +0.1$, the potential is negative in the past.

The equation for evolution of φ (25) can be written in an integral form as

$$\Delta\varphi(z) = -\sqrt{3} M_{\rm Pl} \int_0^z \frac{\sqrt{\Omega_\varphi(z)(1+\omega_\varphi(z))}}{1+z} dz.$$

Since the model depends on $\Delta\varphi$—through $E(z)$—and neither on φ nor on φ_0, then it is independent of φ_0. In other words, φ_0 is not a parameter of the model and can be chosen arbitrarily. Therefore, the parameters of the model are δ, c, h, Ω_{b0}, and $\Omega_{\varphi 0}$.

B. Tachyon scalar field

In the case of dark energy modeled as the tachyon scalar field, $\mathcal{L}_\varphi(x)$ in the action (1) is given by (4). From a variational principle, we obtain

$$i\gamma^\mu \nabla_\mu \Psi - M^* \Psi = 0, \tag{27}$$

$$i(\nabla_\mu \bar\Psi)\gamma^\mu + M^* \bar\Psi = 0, \tag{28}$$

where $M^* \equiv M - \beta\varphi$, and

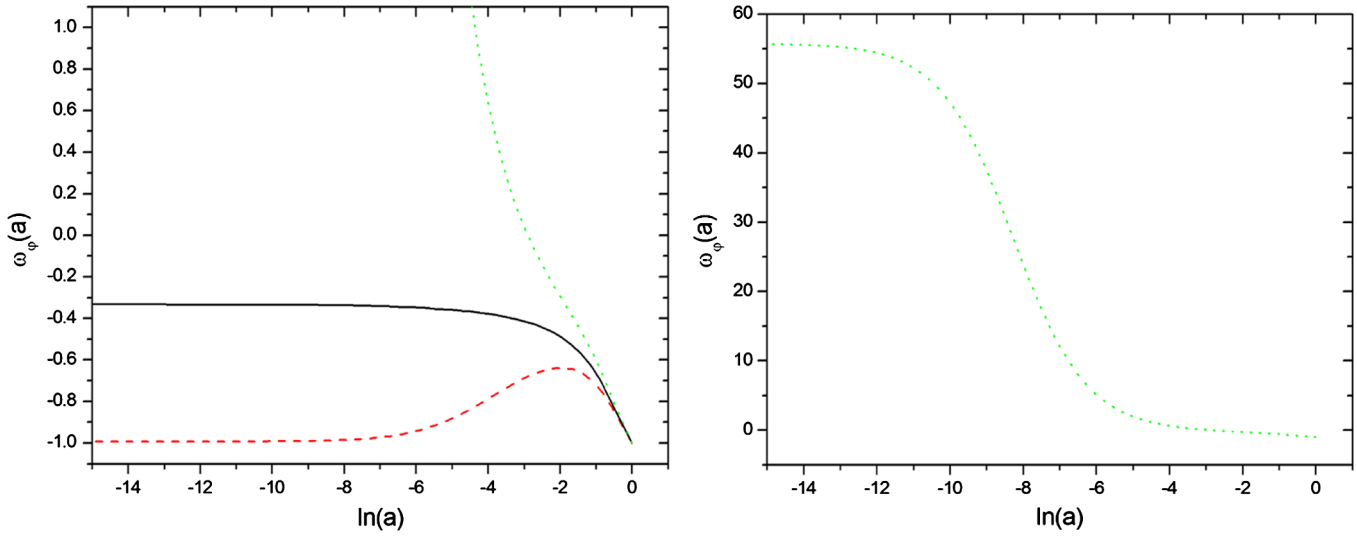

FIG. 1 (color online). Left panel: Equation-of-state parameter of the holographic quintessence model, for $c = 0.85$ and $\delta M_{\rm Pl} = -0.1$ (red dashed line), $\delta M_{\rm Pl} = 0$ (black solid line), and $\delta M_{\rm Pl} = +0.1$ (green dotted line). Right panel: Full range of the equation-of-state parameter for $\delta M_{\rm Pl} = +0.1$.

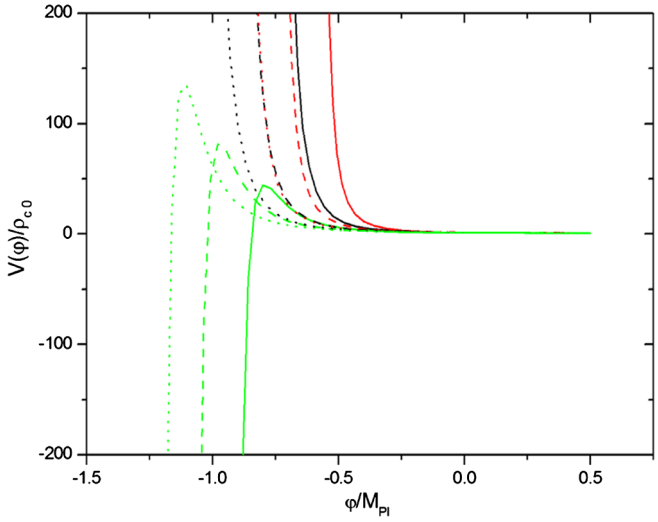

FIG. 2 (color online). Potential of the holographic quintessence field $V(\varphi)$, in units of $\rho_{c0} = 3M_{\rm Pl}^2 H_0^2$. φ is in units of $M_{\rm Pl}$. The solid lines are for $c = 0.95$, the dashed ones are for $c = 1.1$, and the dotted are for $c = 1.25$. For each value of c, the curves from right to left are for $\delta M_{\rm Pl} = -0.1$ (red), $\delta M_{\rm Pl} = 0$ (black), and $\delta M_{\rm Pl} = +0.1$ (green), respectively.

$$\nabla_\mu \partial^\mu \varphi + \alpha \frac{\partial^\mu \varphi (\nabla_\mu \partial_\sigma \varphi) \partial^\sigma \varphi}{1 - \alpha \partial_\mu \varphi \partial^\mu \varphi} + \frac{1}{\alpha} \frac{dlnV(\varphi)}{d\varphi} = \frac{\beta \bar{\Psi}\Psi}{\alpha V(\varphi)} \sqrt{1 - \alpha \partial^\mu \varphi \partial_\mu \varphi}. \quad (29)$$

Equations (27) and (28) are the interacting covariant Dirac equation and its adjoint, respectively, i.e., (27) and (28) are almost the same as Eqs. (5) and (6), the only difference is that the scalar field φ in M^* now is the tachyon field. For homogeneous fields and adopting the flat Friedmann-Robertson-Walker metric, (29) reduces to

$$\ddot{\varphi} = -(1 - \alpha \dot{\varphi}^2) \left[\frac{1}{\alpha} \frac{dlnV(\varphi)}{d\varphi} + 3H\dot{\varphi} - \frac{\beta \bar{\Psi}\Psi}{\alpha V(\varphi)} \sqrt{1 - \alpha \dot{\varphi}^2} \right], \quad (30)$$

whereas for the fermions, the equations of motion will reduce to Eq. (8), as already obtained above.

From the energy-momentum tensor, we get

$$\rho_\varphi = \frac{V(\varphi)}{\sqrt{1 - \alpha \dot{\varphi}^2}}, \quad (31)$$

$$P_\varphi = -V(\varphi) \sqrt{1 - \alpha \dot{\varphi}^2}, \quad (32)$$

$$\rho_\Psi = M^* \bar{\Psi}\Psi,$$

$$P_\Psi = 0.$$

From (31) and (32), we have $\omega_\varphi \equiv \frac{P_\varphi}{\rho_\varphi} = \alpha \dot{\varphi}^2 - 1$. Differentiating (31) and (32) with respect to time and using (30) and (8), we get

$$\dot{\rho}_\varphi + 3H\rho_\varphi(\omega_\varphi + 1) = \beta \dot{\varphi} \bar{\Psi}_0 \Psi_0 \left(\frac{a_0}{a} \right)^3 \quad (33)$$

and

$$\dot{\rho}_\Psi + 3H\rho_\Psi = -\beta \dot{\varphi} \bar{\Psi}_0 \Psi_0 \left(\frac{a_0}{a} \right)^3, \quad (34)$$

where the dot represents derivative with respect to time.

For baryonic matter and radiation, the conservation equations are the same as in the quintessence model. We have (15) and (16) where $\omega_r = \frac{1}{3}$. The Friedmann equation for a flat universe reads

$$H^2 = \frac{1}{3M_{\rm Pl}^2} \left[M^* \bar{\Psi}_0 \Psi_0 \left(\frac{a_0}{a} \right)^3 + \frac{V(\varphi)}{\sqrt{1 - \alpha \dot{\varphi}^2}} + \frac{\rho_{b0}}{a^3} + \frac{\rho_{r0}}{a^4} \right]. \quad (35)$$

Now, as done in the case of the quintessence field, we will identify the tachyon energy density (31) with the holographic dark energy density $\rho_\Lambda = 3c^2 M_{\rm Pl}^2 L^{-2}$. From a similar reasoning, we obtain again the Eqs. (18)–(20). Moreover, we obtain

$$\dot{r} = 3Hr\omega_\varphi - {\rm sign}[\dot{\varphi}] \times \frac{\beta(1+r)^2 \sqrt{1+\omega_\varphi}}{3M_{\rm Pl}^2 \sqrt{\alpha} H^2} \bar{\Psi}_0 \Psi_0 \left(\frac{1+z}{1+z_0} \right)^3, \quad (36)$$

with $r \equiv \frac{\rho_\Psi}{\rho_\varphi}$. As before, the sign of $\dot{\varphi}$ is arbitrary. Also, we can rewrite $\bar{\Psi}_0 \Psi_0$ in terms of observable quantities. We get $M \bar{\Psi}_0 \Psi_0 = \frac{3M_{\rm Pl}^2 H_0^2 (1 - \Omega_{\phi 0} - \Omega_{b0} - \Omega_{r0})}{1 - \frac{\beta}{M\sqrt{\alpha}} \phi_0}$, where we defined $\phi \equiv \sqrt{\alpha}\varphi$. Using (18)–(20), we obtain, after some algebra

$$\omega_\phi(z) = -\frac{1}{3} - \frac{2\sqrt{\Omega_\phi(z)}}{3c} + \frac{\gamma(z)}{3} \left[\gamma(z) + \sqrt{\gamma(z)^2 + 4\left(1 - \frac{\sqrt{\Omega_\phi(z)}}{c} \right)} \right], \quad (37)$$

where

$$\gamma(z) \equiv \frac{1}{\sqrt{6}} \frac{\delta}{H_0} \frac{1 - \Omega_{\phi 0} - \Omega_{b0} - \Omega_{r0}}{\Omega_\phi(z) E^3(z)} \left(\frac{1+z}{1+z_0} \right)^3, \quad (38)$$

with

$$E(z) \equiv \frac{H(z)}{H_0} = \sqrt{\frac{[(1 - \delta\Delta\phi)(1 - \Omega_{\phi 0} - \Omega_{b0} - \Omega_{r0}) + \Omega_{b0}]}{1 - \Omega_\phi} \left(\frac{1+z}{1+z_0} \right)^3 + \frac{\Omega_{r0}}{1 - \Omega_\phi} \left(\frac{1+z}{1+z_0} \right)^4}, \quad (39)$$

where $\Delta\phi(z) \equiv \phi(z) - \phi_0$ and $\delta \equiv \frac{\frac{\beta}{M\sqrt{\alpha}}}{1-\frac{\beta}{M\sqrt{\alpha}}\phi_0}$ is an effective coupling constant. As in the quintessence field case, if $\delta = 0$, (37) reproduces the equation-of-state parameter obtained in [18].

The evolution of the tachyon scalar field is given by

$$\frac{d\phi}{dz} = -\frac{\sqrt{1+\omega_\phi(z)}}{H_0 E(z)(1+z)}. \tag{40}$$

From (18)–(20) and (40), we can calculate the evolution with redshift of all observables in the model. If we wish to calculate the time dependence, we need to integrate the Friedmann Eq. (35), which can be written in the form

$$\frac{dt}{dz} = -\frac{1}{H_0 E(z)(1+z)}.$$

From (31), we can compute the potential $V(z)$ as

$$\frac{V(z)}{\rho_{c0}} = E^2(z)\Omega_\phi(z)\sqrt{-\omega_\phi(z)}, \tag{41}$$

where $\rho_{c0} = 3M_{\rm Pl}^2 H_0^2$, $E(z)$ is given by (39), $\omega_\phi(z)$ is given by (37), and $\Omega_\phi(z)$ is the solution of (18). From (41) and (40), we can compute $V(\phi)$.

The square root in (37) must be real. Furthermore, in analogous manner to the quintessence model, ω_ϕ must be more than -1 because (40). We can verify that ω_ϕ is real and $\omega_\phi > -1$ if (i) $\frac{\sqrt{\Omega_{\phi 0}}}{c} < 1$ or (ii) $\frac{\sqrt{\Omega_{\phi 0}}}{c} > 1$ and $\frac{|\delta|}{H_0} > 2\sqrt{6}\frac{\Omega_{\phi 0}}{1-\Omega_{\phi 0}-\Omega_{b0}-\Omega_{r0}}\sqrt{\frac{\sqrt{\Omega_{\phi 0}}}{c}-1}$. However, the case (ii) is irrelevant, as it corresponds to large values of $\frac{|\delta|}{H_0}$. For example, if $\Omega_{\phi 0} = 0.7$ and $c = 0.8$, we have $\frac{|\delta|}{H_0} \gtrsim 2.45$. Below, we will see that the observational data constrain $\frac{|\delta|}{H_0} \sim 10^{-1}$. As in the quintessence case, because (i) it is necessary that $c \geq 1$ in order that ω_ϕ be real for all future times. This is also the condition for the entropy to increase for all future times, so the tachyon model also respects the second law of thermodynamics.

The evolution of the equation-of-state parameter ω_ϕ is shown in Fig. 3. We have $\omega_\phi \to -1/3$ for $z \gg 1$. In the noninteracting case—$\delta = 0$—this occurs simply because $\Omega_\phi(z) \ll 1$ in high redshifts. The behavior for the interacting case—$\delta \neq 0$—is explained as follows. In the matter era, $E^2(z) \sim (1+z)^3$ so that $\gamma(z) \sim \frac{1}{\Omega_\phi(z)(1+z)^{1.5}}$. Using (18), we infer $\frac{d|\gamma(z)|}{dz} > 0$, that is, $|\gamma(z)|$ increases with redshift z. Therefore, if $\delta < 0$ then $\gamma(z) < 0$ and ω_ϕ increases slower than in the noninteracting case. If $\delta > 0$, then $\gamma(z) > 0$ and ω_ϕ increases faster than in the noninteracting case. In the radiation era, $\gamma(z) \sim \frac{1}{1+z}$ and it turns out to be negligible, so that $\omega_\phi \simeq -1/3$.

In Fig. 4, $V(\phi)$ is shown for some values of δ and c. Notice that—as in the case of the quintessence field potential—$V(\phi)$ possesses a slow-roll region and ϕ evolves to it.

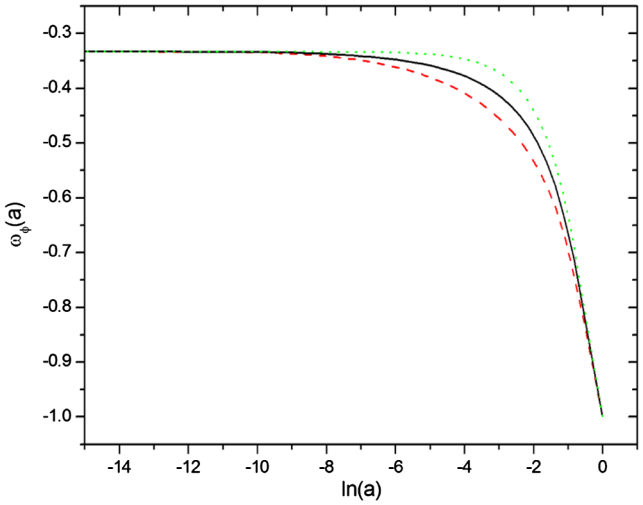

FIG. 3 (color online). Equation-of-state parameter of the holographic tachyon model, for $c = 0.85$ and $\frac{\delta}{H_0} = -0.1$ (red dashed line), $\frac{\delta}{H_0} = 0$ (black solid line), and $\frac{\delta}{H_0} = +0.1$ (green dotted line).

The equation for evolution of ϕ (40) can be written in an integral form as

$$\Delta\phi = -\frac{1}{H_0}\int_0^z \frac{\sqrt{1+\omega_\phi(z)}}{E(z)(1+z)}dz.$$

As before, the model depends on $\Delta\phi$, that is, ϕ_0 is not a parameter. Therefore, the parameters of the model are δ, c, h, Ω_{b0}, and $\Omega_{\phi 0}$. Below, we discuss the comparison with observational data and the results obtained.

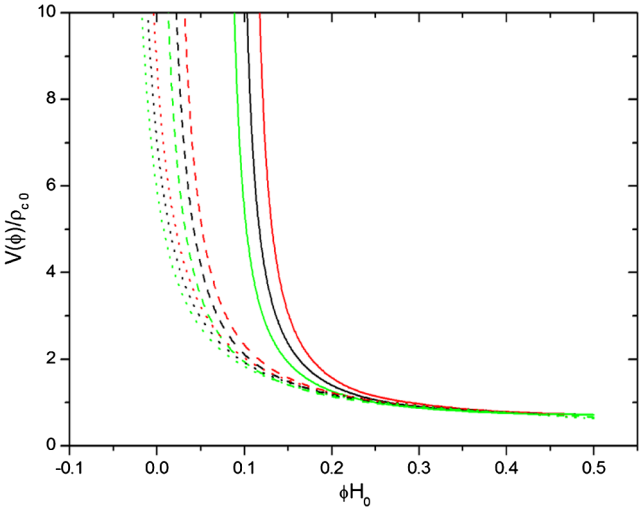

FIG. 4 (color online). Potential of the holographic tachyon field $V(\phi)$, in units of $\rho_{c0} = 3M_{\rm Pl}^2 H_0^2$. ϕ is in units of H_0^{-1}. The solid lines are for $c = 0.85$, the dashed ones are for $c = 1.1$, and the dotted are for $c = 1.35$. For each value of c, the curves from right to left are for $\frac{\delta}{H_0} = -0.1$ (red), $\frac{\delta}{H_0} = 0$ (black), and $\frac{\delta}{H_0} = +0.1$ (green), respectively.

III. CONSTRAINTS FROM OBSERVATIONAL DATA

In [19], the lookback time method has been discussed. Given an object i at redshift z_i, its age $t(z_i)$ is defined as the difference between the age of the Universe at z_i and the age of the Universe at the formation redshift of the object, z_F, that is,

$$t(z_i) = H_0^{-1}\left[\int_{z_i}^{\infty}\frac{dz'}{(1+z')E(z')} - \int_{z_F}^{\infty}\frac{dz'}{(1+z')E(z')}\right] = H_0^{-1}\int_{z_i}^{z_F}\frac{dz'}{(1+z')E(z')} = t_L(z_F) - t_L(z_i), \quad (42)$$

where t_L is the lookback time, given by

$$t_L(z) = H_0^{-1}\int_0^z \frac{dz'}{(1+z')E(z')}.$$

Using (42), the observational lookback time $t_L^{\rm obs}(z_i)$ is

$$t_L^{\rm obs}(z_i) = t_L(z_F) - t(z_i) = [t_0^{\rm obs} - t(z_i)] - [t_0^{\rm obs} - t_L(z_F)] = t_0^{\rm obs} - t(z_i) - df, \quad (43)$$

where $t_0^{\rm obs}$ is the estimated age of the Universe today and df is the delay factor,

$$\mathrm{df} \equiv t_0^{\rm obs} - t_L(z_F).$$

We now minimize χ_L^2,

$$\chi_L^2 = \sum_{i=1}^{N}\frac{[t_L(z_i,\vec{p}) - t_L^{\rm obs}(z_i)]^2}{\sigma_i^2 + \sigma_{t_0^{\rm obs}}^2},$$

where $t_L(z_i,\vec{p})$ is the theoretical value of the lookback time (L) in z_i, $\vec{p}$ denotes the theoretical parameters, $t_L^{\rm obs}(z_i)$ is the corresponding observational value given by (43), σ_i is the uncertainty in the estimated age $t(z_i)$ of the object at z_i, which appears in (43), and $\sigma_{t_0^{\rm obs}}$ is the uncertainty in getting $t_0^{\rm obs}$. The delay factor df appears because of our ignorance about the redshift formation z_F of the object and has to be adjusted. Note, however, that the theoretical lookback time does not depend on this parameter, and we can marginalize over it.

In [20,21], the ages of 35 and 32 red galaxies are, respectively, given. For the age of the Universe, one can adopt $t_0^{\rm obs} = 13.75 \pm 0.11$ Gyr [22]. Although this estimate for $t_0^{\rm obs}$ has been obtained assuming a cosmological constant with cold dark matter (ΛCDM) universe, it does not introduce systematical errors in the calculation: any systematical error eventually introduced here would be compensated by the adjustment of df, in (43). On the other hand, such an estimate is in perfect agreement with other estimates, which are independent of the cosmological model, as, for example, $t_0^{\rm obs} = 12.6^{+3.4}_{-2.4}$ Gyr, obtained from globular cluster ages [23] and $t_0^{\rm obs} = 12.5 \pm 3.0$ Gyr, obtained from radioisotopes studies [24].

The WMAP distance information used by the WMAP Collaboration includes the "shift parameter" R, the "acoustic scale" l_A, and the redshift of decoupling z_*. These quantities are very weakly model dependent [25]. R and l_A are given by

$$R = \sqrt{\Omega_{m0}}H_0 r(z_*)$$

and

$$l_A = \pi\frac{r(z_*)}{r_s(z_*)},$$

where $r(z_*)$ is the comoving distance to z_* and $r_s(z_*)$ is the comoving sound horizon at z_*. For a flat universe, $r(z_*)$ and $r_s(z_*)$ are given by

$$r(z_*) = \frac{1}{H_0}\int_0^{z_*}\frac{dz}{E(z)}$$

and

$$r_s(z_*) = \frac{1}{H_0}\int_0^{z_*}\frac{dz}{E(z)\sqrt{3(1+\bar{R}_b/(1+z))}},$$

where $\bar{R}_b = 3\Omega_{b0}/(4\Omega_{\gamma 0})$. For the redshift of decoupling z_*, we use the fitting function proposed by Hu and Sugiyama [26]:

$$z_* = 1048[1 + 0.001\,24(\Omega_{b0}h^2)^{-0.738}][1 + g_1(\Omega_{m0}h^2)^{g_2}],$$

where

$$g_1 = \frac{0.0783(\Omega_{b0}h^2)^{-0.238}}{1 + 39.5(\Omega_{b0}h^2)^{0.763}}$$

and

$$g_2 = \frac{0.560}{1 + 21.1(\Omega_{b0}h^2)^{1.81}}.$$

Thus, we add to χ^2 the term

$$\chi^2_{\rm CMB} = \sum_{ij}(x_i^{\rm th} - x_i^{\rm data})(C^{-1})_{ij}(x_j^{\rm th} - x_j^{\rm data}),$$

where $x = (l_A, R, z_*)$ is the parameter vector and $(C^{-1})_{ij}$ is the inverse covariance matrix for the seven-year WMAP distance information [27].

BAO are described in terms of the parameter

$$A = \sqrt{\Omega_M}E(z_{\rm BAO})^{-1/3}\left[\frac{1}{z_{\rm BAO}}\int_0^{z_{\rm BAO}}\frac{dz'}{E(z')}\right]^{2/3},$$

where $z_{\rm BAO} = 0.35$. It has been estimated that $A_{\rm obs} = 0.493 \pm 0.017$ [28]. We thus add to χ^2 the term

$$\chi^2_{\rm BAO} = \frac{(A - A_{\rm obs})^2}{\sigma_A^2}.$$

The BAO distance ratio $r_{\rm BAO} \equiv D_V(z = 0.35)/D_V(z = 0.20) = 1.812 \pm 0.060$, estimated from the joint analysis of the 2dFGRS (Two-Degree Field Galaxy Redshift Survey) and SDSS (Sloan Digital Sky Survey) data [29], has also been included. It was demonstrated in [29] that this quantity is weakly model dependent. The quantity $D_V(z_{\rm BAO})$ is given by

$$D_V(z_{\rm BAO}) = c\left[\frac{z_{\rm BAO}}{H(z_{\rm BAO})}\left(\int_0^{z_{\rm BAO}}\frac{dz'}{H(z')}\right)^2\right]^{1/3}.$$

TABLE I. Values of the holographic quintessence model parameters from lookback time, CMB, BAO, and SNe Ia.

$\delta M_{\rm Pl}$	$-0.170^{+0.067+0.148+0.187}_{-0.072-0.123-0.225}$
c	$0.891^{+0.048+0.134+0.234}_{-0.016-0.028-0.035}$
$\Omega_{\phi 0}$	$0.7733^{+0.0092+0.0162+0.0264}_{-0.0087-0.0217-0.0353}$
Ω_{b0}	$0.0450^{+0.0026+0.0061+0.0089}_{-0.0028-0.0048-0.0066}$
h	$0.687 \pm 0.013 \pm 0.026 \pm 0.039$
$\chi^2_{\rm min}$	550.0

So, we have the contribution

$$\chi^2_{r_{\rm BAO}} = \frac{(r_{\rm BAO} - r^{\rm obs}_{\rm BAO})^2}{\sigma^2_{r_{\rm BAO}}}.$$

Finally, we add the 397 supernovae data from Constitution compilation [30]. Defining the distance modulus

$$\mu(z) = 5\log_{10}\left[c(1+z)\int_0^z \frac{dz'}{E(z')}\right] + 25 - 5\log_{10}H_0,$$

we have the contribution

$$\chi^2_{\rm SN} = \sum_{j=1}^{397} \frac{[\mu(z_j) - \mu_{\rm obs}(z_j)]^2}{\sigma_j^2}.$$

Using the expression $\chi^2 = \chi^2_{\rm L} + \chi^2_{\rm CMB} + \chi^2_{\rm BAO} + \chi^2_{r_{\rm BAO}} + \chi^2_{\rm SN}$, the likelihood function is given by

$$\mathcal{L}(\delta, c, h, \Omega_{b0}, \Omega_{\phi_0}) \propto \exp\left[-\frac{\chi^2(\delta, c, h, \Omega_{b0}, \Omega_{\phi_0})}{2}\right].$$

A. Quintessence field

In Table I, we present the values of the individual best-fit parameters, with respective 1σ, 2σ, and 3σ confidence intervals.

Figure 5 shows the marginalized probability distributions for δ and c. The coupling constant δ is nonvanishing at 2σ confidence level. Figure 6 shows some joint confidence regions of two parameters. Notice the effect of the condition $\omega_\phi \leq 1$ on the positive tail of the probability distribution of δ and also in the confidence regions of δ with other parameters.

B. Tachyon scalar field

In Table II, we present the values of the individual best-fit parameters, with respective 1σ, 2σ, and 3σ confidence intervals.

Figure 7 shows the marginalized probability distributions for δ and c. The coupling constant δ is nonvanishing at more than 3σ confidence level. Figure 8 shows some confidence regions of two parameters for this model.

C. Noninteracting models

For comparison, here we present observational constraints on the parameters of the noninteracting holographic model, as well as on the parameters of the constant equation of state and ΛCDM models.

1. Noninteracting holographic dark energy model

The noninteracting holographic dark energy model is obtained simply taking $\delta = 0$ in any one of the above interacting models. Therefore, the equation of state parameter is given by

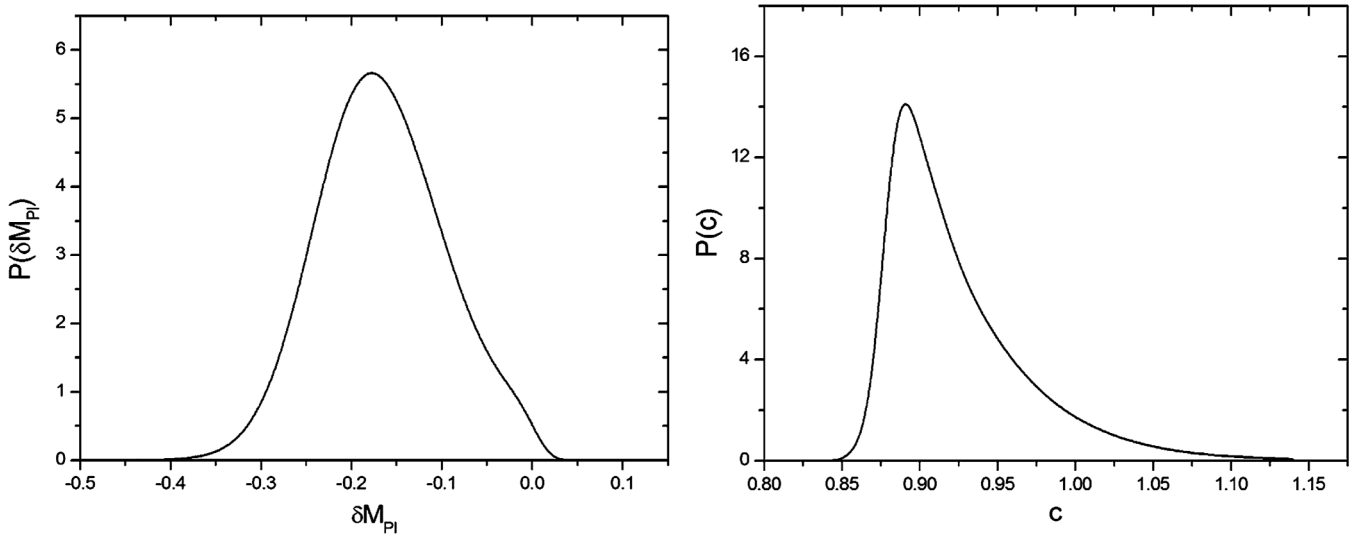

FIG. 5. Probability distributions of the coupling constant δ (left panel) and of the parameter c (right panel) of the holographic quintessence model.

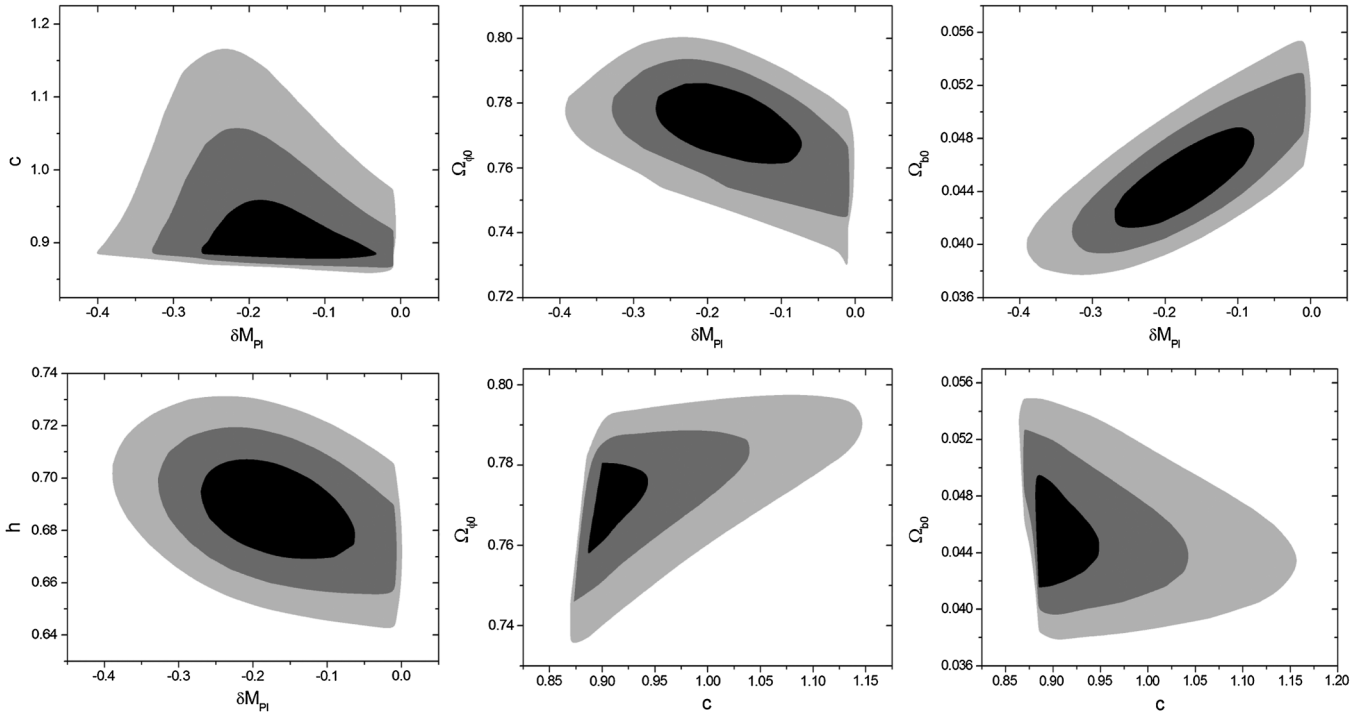

FIG. 6. Two parameters' confidence regions of 1σ, 2σ, and 3σ of the holographic quintessence model.

$$\omega(z) = -\frac{1}{3} - \frac{2\sqrt{\Omega_\varphi(z)}}{3c},$$

as already obtained in [18]. The evolution with redshift of Ω_φ, Ω_b, and Ω_r are given by (18)–(20) and the Friedmann equation can be obtained simply putting $\delta = 0$ in (24) or (39):

$$H(z) = H_0\sqrt{\frac{1-\Omega_{\varphi 0}-\Omega_{r0}}{1-\Omega_\varphi}\left(\frac{1+z}{1+z_0}\right)^3 + \frac{\Omega_{r0}}{1-\Omega_\varphi}\left(\frac{1+z}{1+z_0}\right)^4}. \quad (44)$$

The Table III below presents the constraints on the parameters of the noninteracting holographic model.

2. Constant equation of state and ΛCDM models

If the dark energy possesses a constant equation-of-state parameter, $\omega = \text{const}$, its energy density $\rho_{\rm de}$ is given by

$$\rho_{\rm de}(z) = \rho_{\rm de0}\left(\frac{1+z}{1+z_0}\right)^{3(1+\omega)}, \quad (45)$$

while matter (dark matter and baryonic matter) and radiation are given by $\rho_m(z) = \rho_{m0}(\frac{1+z}{1+z_0})^3$ and $\rho_r(z) = \rho_{r0}(\frac{1+z}{1+z_0})^4$, respectively. The Friedmann equation is

$$H(z) = H_0\sqrt{\Omega_{\rm de0}\left(\frac{1+z}{1+z_0}\right)^{3(1+\omega)} + (1-\Omega_{\rm de0}-\Omega_{r0})\left(\frac{1+z}{1+z_0}\right)^3 + \Omega_{r0}\left(\frac{1+z}{1+z_0}\right)^4}. \quad (46)$$

Notice that the ΛCDM model is a particular case of Eqs. (45) and (46) with $\omega = -1$. Also, it is interesting to notice that, using $\Omega_{\rm de}(z) = (\frac{H_0}{H})^2\Omega_{\rm de0}(\frac{1+z}{1+z_0})^{3(1+\omega)}$, Eq. (46) can be rewritten as (44), that is, (44) is not a particular form of Friedmann equation for the noninteracting holographic model.

The Tables IV and V below present the observational constraints on the parameters of the $\omega = \text{const}$ and ΛCDM models, respectively.

IV. DISCUSSION AND CONCLUSIONS

The minimum χ^2 values in Tables I to V indicate that the tachyon model fits better the observational data. The dimensionless coupling constants, $\delta M_{\rm Pl}$ for the quintessence field and $\frac{\delta}{H_0}$ for the tachyon, agree at 1σ level. Furthermore, both the results imply in dark energy decaying into dark matter, alleviating the coincidence problem. However, whereas for the interacting holographic tachyon model the $\chi^2_{\rm min}$ improves sensibly in comparison with the noninteracting holographic model ($\Delta\chi^2_{\rm min} = -7.8$), for the interacting quintessence holographic model the $\chi^2_{\rm min}$ increases 9.7 in comparison with the noninteracting model. This is a problematic result, as the noninteracting model is a particular case with $\delta = 0$ of the interacting quintessence model. Therefore, if the introduction of δ worsens the fit,

TABLE II. Values of the holographic tachyon model parameters from lookback time, CMB, BAO, and SNe Ia.

$\frac{\delta}{H_0}$	$-0.201^{+0.063+0.117+0.176}_{-0.059-0.138-0.249}$
c	$0.868^{+0.059+0.165+0.235}_{-0.020-0.030-0.038}$
$\Omega_{\phi 0}$	$0.724^{+0.013+0.025+0.036}_{-0.012-0.026-0.040}$
Ω_{b0}	$0.0480 \pm 0.0021 \pm 0.0041 \pm 0.0062$
h	$0.669 \pm 0.012 \pm 0.025 \pm 0.037$
$\chi^2_{\min}$	532.5

TABLE III. Values of the noninteracting holographic model parameters from lookback time, CMB, BAO, and SNe Ia.

c	$0.867^{+0.023+0.061+0.124}_{-0.013-0.019-0.029}$
$\Omega_{\phi 0}$	$0.7362^{+0.0090+0.0178+0.0267}_{-0.0083-0.0183-0.0292}$
Ω_{b0}	$0.0512 \pm 0.0018 \pm 0.0035 \pm 0.0053$
h	$0.667 \pm 0.011 \pm 0.022 \pm 0.033$
$\chi^2_{\min}$	540.3

so δ should be compatible with zero. However, as we can see in Table I, δ is different from zero with more than 2σ confidence level for the quintessence model. This result could be an effect of the condition $\omega_\phi \leq 1$, needed to avoid unphysical negative values of the quintessence potential. In fact, as already discussed above, the condition $\omega_\phi \leq 1$ cuts the $\delta > 0$ region of the probability distribution. This could explain the fact that δ turned out to be different from zero for the quintessence model. In any manner, from the $\chi^2_{\min}$ values in Tables I to V, we see that the interacting quintessence model was disfavored by the data in comparison with the others models considered here.

In Tables IV and V, we see that the $\chi^2_{\min}$ for the $\omega =$ const and for the ΛCDM models are almost the same and the value $\omega = -1.024 \pm 0.049$ is consistent with the ΛCDM ($\omega = -1$) value. From the Tables III, IV, and V, we see that the $\omega =$ const and the ΛCDM models fit better the data than the noninteracting holographic model—$\Delta\chi^2_{\min} = -5.2$ and $\Delta\chi^2_{\min} = -4.7$, respectively. As the $\omega =$ const and the noninteracting holographic models have the same number of parameters, $\Delta\chi^2_{\min} = -5.2$ would signify that the last is disfavored by 2.3σ in relation to the former, if the posterior was Gaussian. As the noninteracting holographic model possesses one more parameter than the ΛCDM, this is disfavored by much more than 2σ in relation to the ΛCDM. On the other hand, the interacting holographic tachyon model fits the data better than the ΛCDM-$\Delta\chi^2_{\min} = -3.1$. Moreover, δ is different from zero with more than 3σ confidence level for the tachyon model, see Table II. However, this is not a true evidence of interaction. In fact, as the noninteracting holographic model is a bad fit to the combination of data sets considered in this work as compared with the ΛCDM, the new parameter—the coupling constant—is needed in order to improve the holographic model. We can see this more clearly if we compare the interacting holographic tachyon and the noninteracting holographic models. The last is a particular case of the former with zero coupling constant. The introduction of the coupling constant reduces $\chi^2_{\min}$ of 7.8 and the coupling constant results nonvanishing with more than 3σ. If the posterior was Gaussian, $\Delta\chi^2_{\min} = -7.8$ would be formally a 2.8σ effect. But, the posterior is non-Gaussian, as we can see in Fig. 7, so the fact that the coupling constant is nonvanishing with more than 3σ is completely understood.

It is interesting to compare the results obtained in the present work for the holographic tachyon model with the previous ones, presented in [6], where a simpler version of

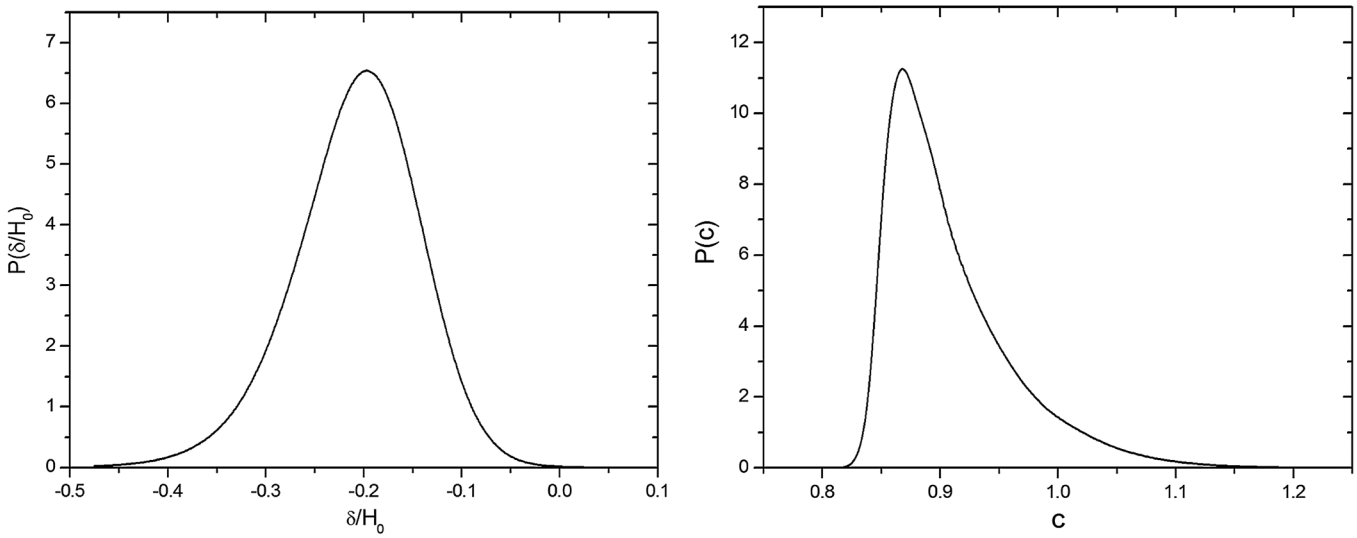

FIG. 7. Probability distributions of the coupling constant δ (left panel) and of the parameter c (right panel) of the holographic tachyon model.

TABLE IV. Values of the $\omega =$ const model parameters from lookback time, CMB, BAO, and SNe Ia.

ω	$-1.024 \pm 0.049 \pm 0.098 \pm 0.147$
Ω_{de0}	$0.7306 \pm 0.0096 \pm 0.0193 \pm 0.0289$
Ω_{b0}	$0.0471 \pm 0.0018 \pm 0.0037 \pm 0.0055$
h	$0.685 \pm 0.013 \pm 0.026 \pm 0.038$
χ^2_{min}	535.1

TABLE V. Values of the ΛCDM model parameters from lookback time, CMB, BAO, and SNe Ia.

Ω_{de0}	$0.7385 \pm 0.0084 \pm 0.0167 \pm 0.0251$
Ω_{b0}	$0.0474 \pm 0.0016 \pm 0.0033 \pm 0.0049$
h	$0.684 \pm 0.012 \pm 0.023 \pm 0.035$
χ^2_{min}	535.6

the holographic tachyon model, without baryons or radiation, had been compared with observational data. The values obtained here for c, $\Omega_{\phi 0}$, and h are the same as before and have smaller confidence intervals, despite the fact that here we have one more parameter—Ω_{b0}—as we can see by comparing Table II in the present work with Table 1 in [6]. This is because now it was possible to use all WMAP distance information R, l_A, and z_*, as the model was generalized to include baryons and radiation. However, the dark energy coupling constant δ now is nonvanishing and compatible with dark energy decaying into dark matter with more than 3σ confidence level, whereas in [6] it was compatible with zero. This can be understood as follows. In low redshifts, the Universe is dominated by dark energy. The dynamics of dark energy in low redshifts is essentially determined by the equation-of-state parameter $\omega_\phi(z)$, as can be seen in (18). As in this period the data sets were the same in both the works, so $\omega_\phi(z)$ must be almost the same in this period in both the works. But, $\omega_\phi(z)$ explicitly depends on the product $\delta\Omega_{\Psi 0}$, were δ is the coupling constant and $\Omega_{\Psi 0} = 1 - \Omega_{\varphi 0} - \Omega_{b0} - \Omega_{r0}$ is the dark matter relative density, as we can see in (37) and (38). As in the present work $\Omega_{\Psi 0}$ is less than that in [6]—where $\Omega_{b0} = \Omega_{r0} \equiv 0$—it turns out that δ in the present work is bigger (in modulus) than that in [6].

The results obtained for c, Ω_{b0}, and h for the three holographic models agree at 1σ confidence level. The value of $\Omega_{\phi 0}$ for the quintessence model agrees only at 2σ level with the values for the tachyon and the noninteracting models. For the quintessence model, $\Omega_{\phi 0}$ is almost superestimated, corresponding to a matter relative density today $\Omega_{m0} = 0.2267^{+0.0087+0.0217}_{-0.0092-0.0162}$. This value agrees only at 2σ level with the cosmological model independent estimative $\Omega_{\mathrm{Mobs}} = 0.28 \pm 0.04$ [31]. For the noninteracting and tachyon holographic models, we have $\Omega_{m0} = 0.2638^{+0.0083}_{-0.0090}$ and $\Omega_{m0} = 0.276^{+0.012}_{-0.013}$, respectively, both in perfect agreement with that observational estimative. For the three holographic models, the baryon density and the Hubble parameter today are very reasonable. We have obtained $\Omega_{b0}h^2 = 0.0228 \pm 0.0011$, $\Omega_{b0}h^2 = 0.0212 \pm 0.0015$, and $\Omega_{b0}h^2 = 0.0215 \pm 0.0012$ from noninteracting, quintessence, and tachyon holographic models, respectively. Let us compare these values, for example, with that obtained from deuterium to hydrogen abundance ratio [32], $\Omega_{b0}h^2 = 0.0213 \pm 0.0013 \pm 0.0004$, where the error terms represent the 1σ errors from deuterium to hydrogen abundance ratio and the uncertainties in the nuclear reaction rates, respectively. For the Hubble parameter, we have obtained $h = 0.667 \pm 0.011$, $h = 0.687 \pm 0.013$, and $h = 0.669 \pm 0.012$ from noninteracting, quintessence, and tachyon holographic models, respectively, the three in excellent agreement with observational values, independent of cosmological model, as, for example, $h_{\mathrm{obs}} = 0.69 \pm 0.12$ [20] and $h_{\mathrm{obs}} = 0.72 \pm 0.08$ [33]. We can also compare the ratios $\Omega_{b0}/\Omega_{m0} = 0.241^{+0.015}_{-0.014}$, from the noninteracting holographic model, $\Omega_{b0}/\Omega_{m0} = 0.248^{+0.022}_{-0.023}$, from the quintessence model, and $\Omega_{b0}/\Omega_{m0} = 0.211 \pm 0.016$, from the tachyon model, with the observational value of 2dFGRS Collaboration, $\Omega_{b0}/\Omega_{m0} = 0.185 \pm 0.046$ [34].

As already discussed above, it is necessary that $c \geq 1$ in order that the equation-of-state parameter ω_ϕ of the interacting models be real for all future times, but we have obtained $c < 1$ at 1σ confidence level for both interacting models. However, this is not a very serious problem, because c is compatible with values above unity at 2σ confidence level. Moreover, one could say that $c < 1$ is only an effect due to lack of more precise observational data. Anyway, the very simple models presented here are expected to be only alternatives to an effective description of a more sophisticated subjacent theory of dark energy. In principle, nothing guarantees that they will be good descriptions for all future times.

Figures 6 and 8 show some joint confidence regions of two parameters for both interacting models. In the confidence regions for δ versus c and for c versus $\Omega_{\phi 0}$, we see that there is a lower limit on $c \approx 0.8$. This also can be seen in the marginalized probability distributions of c, which dies for $c \lesssim 0.85$. This lower limit is explained by the condition $\frac{\sqrt{\Omega_{\phi 0}}}{c} < 1$, necessary for ω_ϕ to be real and $\omega_\phi > -1$, discussed above. This limit can be seen more clearly in c versus $\Omega_{\phi 0}$ confidence regions. Moreover, we have $c \simeq \sqrt{\Omega_{\phi 0}}$ for the best-fit values of these parameters for the three holographic models. This implies that $\omega_{\phi 0} \simeq -1$ and these models approach ΛCDM today. This is consistent with the fact that, as ΛCDM fits all observational data, then any alternative model must not deviate much from ΛCDM for $z \approx 0$. However, for $z > 0$, the three models are qualitatively different from ΛCDM. For the quintessence field, we have very different qualitative behaviors for $\delta < 0$, $\delta = 0$, and $\delta > 0$, as shown in Fig. 1 and discussed in II A. For

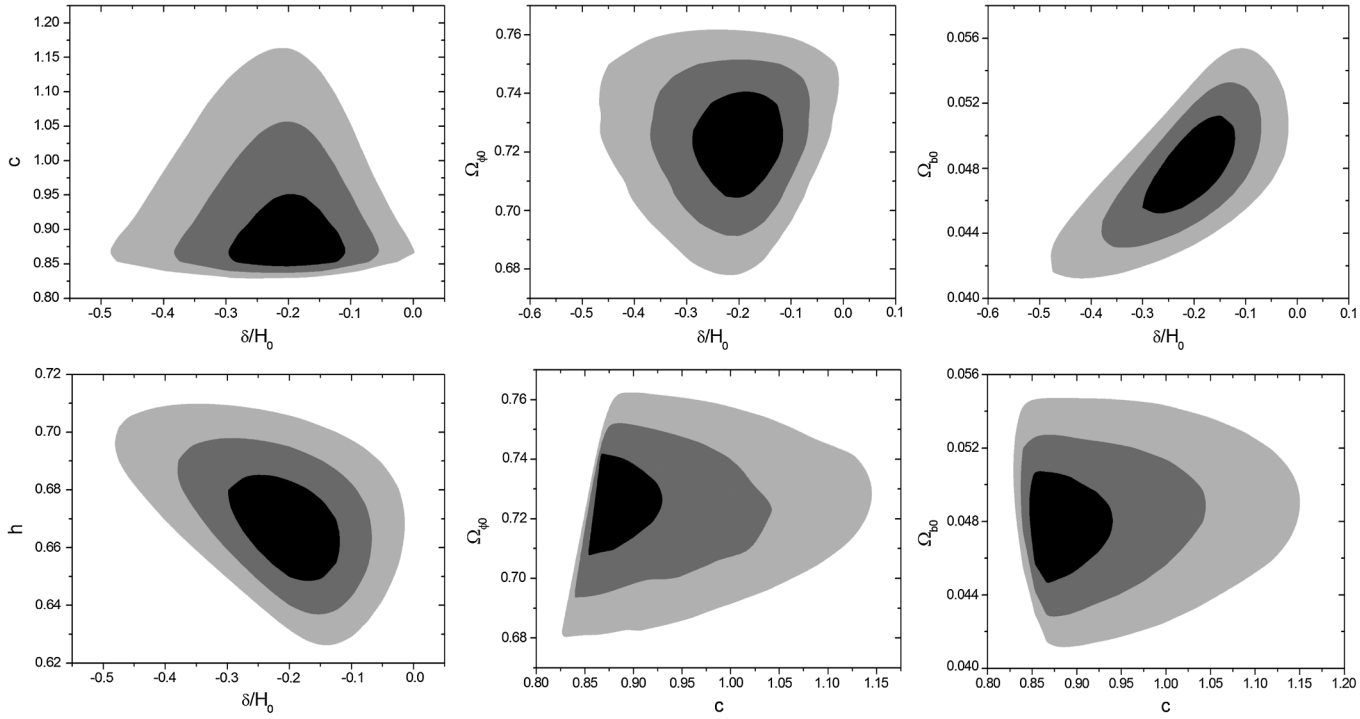

FIG. 8. Two parameters' confidence regions of 1σ, 2σ, and 3σ of the holographic tachyon model.

the tachyon model, its behavior is qualitatively the same in the three cases, ω_ϕ approximates $-1/3$, as shown in Fig. 3 and discussed in II B. The behavior for the noninteracting holographic model corresponds to the case $\delta = 0$ in Fig. 1 or in Fig. 3.

In summary, combinations of the holographic dark energy model and interacting scalar fields were implemented. It was shown that it is possible to fix the potential of interacting scalar fields by imposing that the energy density of the scalar field must match the energy density of the holographic dark energy. A comparison of the models with recent observational data was made and the coupling is nonvanishing at more than 2σ for the quintessence field and at more than 3σ for the tachyon. In both cases, the results are consistent with dark energy decaying into dark matter, alleviating the coincidence problem. However, the results for the quintessence model are problematic—the interaction worsens χ^2_{min} with respect to the noninteracting case. On the other hand, the results for the tachyon model are better than that for the ΛCDM ($\Delta\chi^2_{\text{min}} = -3.1$), but this is not a true evidence of interaction, because the noninteracting holographic model is a bad fit to the combination of data sets considered in this work as compared with ΛCDM, so that the new parameter—the coupling constant—is needed in order to improve the holographic model. Therefore, the question about the interaction in the dark sector of the Universe remains open. The comparison with more observational data and possibly the use of more refined techniques, such as the Bayesian evidence test, will be necessary in order to solve this question.

ACKNOWLEDGMENTS

This work has been supported by CNPq (Conselho Nacional de Desenvolvimento Científico e Tecnológico) of Brazil.

[1] W. Zimdahl, D. Pavon, and L. P. Chimento, Phys. Lett. B **521**, 133 (2001); L. P. Chimento, A. S. Jakubi, D. Pavon, and W. Zimdahl, Phys. Rev. D **67**, 083513 (2003).

[2] J.-H. He and B. Wang, J. Cosmol. Astropart. Phys. 06 (2008) 010; C. Feng, B. Wang, E. Abdalla, and R.-K. Su, Phys. Lett. B **665**, 111 (2008); J.-H. He, B. Wang, and E. Abdalla, Phys. Lett. B **671**, 139 (2009).

[3] B. Wang, J. Zang, C.-Y. Lin, E. Abdalla, and S. Micheletti, Nucl. Phys. **B778**, 69 (2007).

[4] S. Micheletti, E. Abdalla, and B. Wang, Phys. Rev. D **79**, 123506 (2009).

[5] B. Gumjudpai, T. Naskar, M. Sami, and S. Tsujikawa, J. Cosmol. Astropart. Phys. 06 (2005) 007; B. Wang, Y.-G. Gong, and E. Abdalla, Phys. Lett. B **624**, 141 (2005);

M. R. Setare, Phys. Lett. B **642**, 1 (2006); Eur. Phys. J. C **50**, 991 (2007); Phys. Lett. B **654**, 1 (2007); E. Abdalla and B. Wang, Phys. Lett. B **651**, 89 (2007); R. Rosenfeld, Phys. Rev. D **75**, 083509 (2007); M. Quartin, M. O. Calvao, S. E. Joras, R. R. R. Reis, and I. Waga, J. Cosmol. Astropart. Phys. 05 (2008) 007; Q. Wu, Y. Gong, A. Wang, and J. S. Alcaniz, Phys. Lett. B **659**, 34 (2008); M. R. Setare and E. C. Vagenas, Phys. Lett. B **666**, 111 (2008); M. Jamil and M. A. Rashid, Eur. Phys. J. C **56**, 429 (2008); **58**, 111 (2008); M. R. Setare and E. C. Vagenas, Int. J. Mod. Phys. D **18**, 147 (2009); X.-M. Chen, Y.-G. Gong, and E. N. Saridakis, J. Cosmol. Astropart. Phys. 04 (2009) 001; Z.-K. Guo, N. Ohta, and S. Tsujikawa, Phys. Rev. D **76**, 023508 (2007); O. Bertolami, F. Gil Pedro, and M. Le Delliou, Phys. Lett. B **654**, 165 (2007); Gen. Relativ. Gravit. **41**, 2839 (2009); L. P. Chimento, Phys. Rev. D **81**, 043525 (2010).

[6] S. Micheletti, J. Cosmol. Astropart. Phys. 05 (2010) 009.

[7] P. J. E. Peebles, *Physical Cosmology* (Princeton University, Princeton, NJ, 1993).

[8] E. Abdalla, L. R. W. Abramo, L. Sodre Jr., and B. Wang, Phys. Lett. B **673**, 107 (2009); E. Abdalla, L. R. W. Abramo, and J. C. C. de Souza, Phys. Rev. D **82**, 023508 (2010).

[9] R. Bean, E. E. Flanagan, I. Laszlo, and M. Trodden, Phys. Rev. D **78**, 123514 (2008).

[10] E. J. Copeland, M. Sami, and S. Tsujikawa, Int. J. Mod. Phys. D **15**, 1753 (2006); M. Sami, Curr. Sci. **97**, 887 (2009).

[11] I. Zlatev, L. Wang, and P. J. Steinhardt, Phys. Rev. Lett. **82**, 896 (1999); P. J. Steinhardt, L. Wang, and I. Zlatev, Phys. Rev. D **59**, 123504 (1999); L. Amendola, Phys. Rev. D **62**, 043511 (2000); R. R. Caldwell and E. V. Linder, Phys. Rev. Lett. **95**, 141301 (2005); R. J. Scherrer and A. A. Sen, Phys. Rev. D **77**, 083515 (2008); A. A. Sen, G. Gupta, and S. Das, J. Cosmol. Astropart. Phys. 09 (2009) 027.

[12] A. Sen, J. High Energy Phys. 04 (2002) 048; 07 (2002) 065; Mod. Phys. Lett. A **17**, 1797 (2002).

[13] T. Padmanabhan, Phys. Rev. D **66**, 021301 (2002); A. Feinstein, Phys. Rev. D **66**, 063511 (2002); J. S. Bagla, H. K. Jassal, and T. Padmanabhan, Phys. Rev. D **67**, 063504 (2003); L. R. W. Abramo and F. Finelli, Phys. Lett. B **575**, 165 (2003); R. Herrera, D. Pavon, and W. Zimdahl, Gen. Relativ. Gravit. **36**, 2161 (2004); A. Ali, M. Sami, and A. A. Sen, Phys. Rev. D **79**, 123501 (2009).

[14] J. Zhang, X. Zhang, and H. Liu, Phys. Lett. B **651**, 84 (2007); M. R. Setare, Phys. Lett. B **653**, 116 (2007).

[15] X. Zhang, Phys. Lett. B **648**, 1 (2007).

[16] X. Zhang, Phys. Rev. D **74**, 103505 (2006).

[17] T. Damour, G. W. Gibbons, and C. Gundlach, Phys. Rev. Lett. **64**, 123 (1990).

[18] M. Li, Phys. Lett. B **603**, 1 (2004); Q.-G. Huang and M. Li, J. Cosmol. Astropart. Phys. 08 (2004) 013.

[19] S. Capozziello, V. F. Cardone, M. Funaro, and S. Andreon, Phys. Rev. D **70**, 123501 (2004).

[20] R. Jimenez, L. Verde, T. Treu, and D. Stern, Astrophys. J. **593**, 622 (2003).

[21] J. Simon, L. Verde, and R. Jimenez, Phys. Rev. D **71**, 123001 (2005).

[22] N. Jarosik *et al.*, Astrophys. J. Suppl. Ser. **192**, 14 (2011); WMAP Cosmological Parameters Model/Dataset Matrix homepage, http://lambda.gsfc.nasa.gov/product/map/current/best_params.cfm.

[23] L. M. Krauss, arXiv:astro-ph/0301012.

[24] R. Cayrel *et al.*, Nature (London) **409**, 691 (2001).

[25] H. Li, J.-Q. Xia, G.-B. Zhao, Z.-H. Fan, and X. Zhang, Astrophys. J. **683**, L1 (2008); Y. Wang and P. Mukherjee, Phys. Rev. D **76**, 103533 (2007).

[26] W. Hu and N. Sugiyama, Astrophys. J. **471**, 542 (1996).

[27] E. Komatsu *et al.*, Astrophys. J. Suppl. Ser. **192**, 18 (2011).

[28] B. A. Reid *et al.*, Mon. Not. R. Astron. Soc. **404**, 60 (2010).

[29] W. J. Percival, S. Cole, D. J. Eisenstein, R. C. Nichol, J. A. Peacock, A. C. Pope, and A. S. Szalay, Mon. Not. R. Astron. Soc. **381**, 1053 (2007).

[30] M. Hicken, W. M. Wood-Vasey, S. Blondin, P. Challis, S. Jha, P. L. Kelly, A. Rest, and R. P. Kirshner, Astrophys. J. **700**, 1097 (2009).

[31] A. G. Riess *et al.*, Astrophys. J. **659**, 98 (2007).

[32] J. M. O'Meara, S. Burles, J. X. Prochaska, G. E. Prochter, R. A. Bernstein, and K. M. Burgess, Astrophys. J. **649**, L61 (2006).

[33] W. L. Freedman *et al.*, Astrophys. J. **553**, 47 (2001).

[34] S. Cole *et al.*, Mon. Not. R. Astron. Soc. **362**, 505 (2005).